Electronic Supplementary Material (ESI) for Journal of Materials Chemistry A.

Supporting Information

Indanone-based Conjugated Polymers Enabling Ultrafast Electron Transfer for Visible Light-driven Hydrogen Evolution from Water

*Tse-Fu Huang, Ying-Rang Zhuang, Chih-Li Chang, Ching-Li Huang, Wei-Cheng Lin, Zi-Cheng Jiang, Li-Yu Ting, Islam M. A. Mekhemer, Yu-En Sun, Pinit Kidkhunthod, Jeng-Lung Chen, Yi-Chan Huang, Hung-Kai Hsu, Yuan-Ting Tseng, Yi-Hsiang Wu, Bing-Heng Li, Shang-Da Yang, Yen-Ju Cheng and Ho-Hsiu Chou**

General methods: All reagents were obtained from commercial suppliers and were used without further purification. First, 3,7-bis(4,4,5,5-tetramethyl-1,3,2-dioxaborolan-2-yl)dibenzo[b,d]thiophene 5,5-dioxide (DB) was synthesized by following procedures reported in our previous papers.[1] All reactions were performed under a nitrogen atmosphere with standard Schlenk techniques. 1H and 13C NMR spectra were recorded in solution at 500 MHz, using a Bruker Advance 500 MHz NMR spectrometer. Mass spectra were obtained using a AccuTOF GCX HRMS instrument. Fourier-transform infrared (FT-IR) spectra were recorded using a Thermo Scientific iS50 FT-IR infrared spectrometer. Thermogravimetric analysis of the polymers was performed under nitrogen using a TA Q600 instrument over the temperature range of 50–800 °C (heating rate: 10 °C min–1). Powder X-ray diffraction (PXRD) measurements were performed using a Bruker Instruments D2-Phaser equipped with Cu Kα radiation. The HOMO energy levels were measured using Cyclic voltammetry (CV). CV, electrochemical impedance spectroscopy (EIS), and transient photocurrent measurements were performed using a Zahner Zennium E workstation equipped with a three-electrode cell.UV–vis absorption spectra of the polymers were recorded on a Hitachi U-3300 spectrophotometer. The optical bandgap (Eg) was obtained from Tauc plots ((αhn)2 versus (hn)) of the UV-Vis spectra and by extrapolation of the linear part of the curve to the energy axis based on the relationship αhn = A(hn - Eg)γ, where α is the absorption coefficient, A is an energy-independent constant, Eg is the optical band gap, h is Planck's constant, v is the velocity, and γ is a constant representing the type of electronic transition. The LUMO energy levels were calculated by subtracting the Eg from the HOMO energy levels. Time-resolved transient PL decay spectra of the polymer photocatalysts were obtained using an Edinburgh FLS 980 instrument.

Photoelectrochemical measurements.

Photoelectrochemical measurements were conducted using a Zahner Zennium workstation with a three-electrode cell system. The system comprised a platinum wire counter electrode, an FTO glass working electrode, and an Ag/AgCl reference electrode (3M NaCl). A 0.5 M Na2SO4 electrolyte solution was employed. The three polymers were deposited on the working electrode using the drop-casting method with dimethylformide as the solvent. For electrochemical impedance measurements, an AC potential was applied to the electrochemical cell, and the current through the cell was measured. Photocurrent measurements were performed by applying a constant potential of 1.5 V, with 20 seconds of light on-off cycles at specified intervals to record both photo and dark currents under LED light illumination.

Cyclic voltammetry measurements and HOMO calculation.

A standard three electrode cell system was used for the CV experiments. A Pt rod with a 2 mm diameter was used as the working electrode, a Pt mesh electrode was used as the counter electrode and an Ag/AgCl electrode was used as the reference electrode. Ag/AgCl redox potential was determined by pH-dependent formula: ${E^0}_{Ag/AgCl} = 0.1976V + 0.059pH$. The HOMO levels are claculated as follows: $E_{HOMO} =- (E_{ox,onset} - {E^0}_{Ag/AgCl} + 4.44)$ eV.

The apparent quantum yield (AQY).

The entire hydrogen evolution reaction is assumed to be a two-electron process. The AQY values were calculated using the following equation:

$$AQY(\%) = \frac{2 \times the\ number\ of\ produced\ hydrogen\ molecules}{the\ number\ of\ incident\ photons} = \frac{2 \times \hbar \times H \times N_A}{P \times t \times A \times \frac{\lambda}{c}} \times 100\%$$

Here, H is the amount of hydrogen produced (in units of mol), $\hbar$ the Planck constant, N_A the Avogadro constant, A the irradiation area (m^2), P the intensity of the monochromatic light (W m^{-2}), t the time (s), λ the wavelength of the monochromatic light (m), and c the speed of light (m · s^{-1}).

Transient absorption spectroscopy setup.

The measurements were conducted using a commercial Yb:KGW laser system (Pharos, Light Conversion) operating at a central wavelength of 1030 nm. This laser system had an average power output of 2.5 W, a repetition rate of 3.125 kHz, a pulse energy of 800 μJ, and a pulse duration of 190 fs. To generate two identical pulses, a low-GDD 50/50 beam splitter was employed, and both pulses were subsequently directed through our specially designed nonlinear compressor using a well-established technique called multiple plate compression (MPC).[2, 3] For this experiment, we applied a high-pass filter with a cut-off wavelength of 980 nm. Pulse compression was achieved using eight chirped mirror bounces (Ultrafast Innovation), effectively removing material dispersion introduced by the optics before reaching the sample. The compressed pulses had a full width at half maximum (FWHM) duration of 3.2 fs and were characterized at the sample position using polarization-gating frequency-resolved optical gating

(PG-FROG). The pump pulse was modulated by a laser-triggered mechanical chopper operating at half the laser repetition rate (1.5625 kHz). Tunable color filters, consisting of a combination of high-pass and low-pass filters, were used to finely adjust the pumping bandwidth and central wavelength. To precisely control the excitation power and avoid introducing nonlinear effects, we employed a broadband half-wave plate and a wire-grid polarizer. The delay time, relative to the pump pulse, of the probe pulse was adjusted using a linear translation stage (DL325, Newport), providing a delay range of up to approximately 2.2 ns. Both the pump and probe beams were focused onto the sample in a noncollinear manner, with a cross-angle of 5 degrees. Different focusing conditions were selected for the pump and probe pulses to ensure that the focused pump spot size (~67.7 μm) was slightly larger than the focused probe spot size (~27.3 μm), ensuring uniform excitation of the probed region. After passing through the sample, the transmitted probe pulse was spatially separated and directed into our designed spectrometer, which featured a high-speed linear array camera (Glaz Linescan-I-Gen2, Synertronic with S12198-512Q CMOS, Hamamatsu) to capture each probe pulse. Because the pump pulses were modulated at half of the repetition rate, the spectral difference between every two probe shots provided the ΔT/T signal. The supporting information for TAS is provided by Shang-Da Yang's group.[4]

Synthesis of monomers.

Synthesis of 5-bromo-1H-indene-1,3(2H)-dione (ICBrF):

4-bromophthalic anhydride (9.08 g, 40 mmol), triethylamine (11.8 ml), acetic anhydride (21.8 ml) were added to a reaction flask. After completely stirring, ethyl acetoacetate (5.72 ml) was added, followed by stirring at room temperature for 22 h. Then, pour ice water (15.5 ml) into the flask, followed by adding 5M HCl (64 ml) and concentrated HCl (14.5 ml), and the mixture was heated at 80 ℃ for 15 min. Then, the mixture were extracted by dichloromethane and H_2O, dried over anhydrous $MgSO_4$, and concentrated under reduced pressure. The crude product was further purified by recrystallization with acetone to afford ICBrF (6.9 g, 30.8 mmol, yield 77.0%). ^{1}H NMR (500 MHz, CDCl$_3$): δ 8.10 (s, 1H), 7.94 (d, J = 9 Hz, 1H), 7.82 (d, J = 9 Hz, 1H) and 3.23 (s, 2H). ^{13}C NMR (500 MHz, CDCl$_3$): δ 196.08, 195.84, 144.50, 141.75, 138.73, 131.29, 126.42, 125.56 and 44.95. HRMS (FD): calcd for $C_9H_5BrO_2$: 223.9473 [M]$^+$, found: m/z 223.9478.

Synthesis of 2-(5/6-bromo-3-oxo-2,3-dihydro-1H-inden-1-ylidene)malononitrile (ICBr): ICBrF (0.56 g, 2.5 mmol), malononitrile (0.33 g, 5 mmol), sodium acetate (0.31 g, 3.75 mmol) and ethanol (10 ml) were added to a reaction flask, and stirred at room temperature for 1 h. Then, pour H_2O (10 ml) into the flask, followed by adding concentrated HCl (0.125 ml), and keep stirring for 30 min until precipitate occurs . The mixture was filtered through funnel to gain crude product, and further washed with water and n-hexane to afford ICBr (0.425 g, 1.56 mmol, yield 62.2%). ^{1}H NMR (500 MHz, CDCl$_3$): δ 8.75 (s, 1H), 8.49 (d, J = 9 Hz, 1H), 8.09 (s, 1H), 7.98 – 7.94 (m, 2H), 7.82 (d, J = 9 Hz, 1H) and 3.72 (s, 4H). ^{13}C NMR (500 MHz, CDCl$_3$): δ 193.49, 193.33, 164.92, 164.56, 143.61, 141.64, 140.88, 139.10, 139.01, 138.88, 131.74, 131.53, 128.85, 127.92, 127.01, 125.69, 112.00, 111.83, 111.62, 80.41, 79.58, 43.18 and 43.15. HRMS (FD): calcd for $C_{12}H_5BrN_2O$: 271.9585 [M]$^+$, found: m/z 271.9591.

Synthesis of 2,2'-(5-bromo-1H-indene-1,3(2H)-diylidene)dimalononitrile (IDMBr): A reaction flask with ICBrF (2.24 g, 10 mmol), malononitrile (1.98 g, 30 mmol), ammonium acetate (0.77 g, 10 mmol) and ethanol (20 ml) was refluxed at 99 ℃ under a nitrogen atmosphere for 24 h. The ethanol was removed by rotary evaporator followed by adding H_2O. The concentrated hydrochloric acid was added, keep stirring solution at 60 ℃ to completely protonate the product. The mixture were extracted by chloroform and H_2O, while adding more hydrochloric acid. The extract was dried over anhydrous $MgSO_4$, and concentrated under reduced pressure to afford IDMBr (2.47 g, 7.73 mmol, yield 77.3%). ^{1}H NMR (500 MHz,

$CDCl_3$): δ8.73 (s, 1H), 8.47 (d, J = 9 Hz, 1H), 7.99 (d, J = 9 Hz, 1H) and 4.27 (s, 1H). ^{13}C NMR (500 MHz, $CDCl_3$): δ 163.95, 163.65, 141.64, 139.39, 139.04, 132.11, 129.74, 127.51, 111.57, 111.38, 111.35, 111.02, 80.44, 79.55 and 41.81. HRMS (ESI): calcd for $C_{15}H_5BrN_4$: 318.9625 $[M - H]^-$, found: m/z 318.9622.

General procedure for Suzuki-Miyaura coupling polymerization.

A mixture comprising monomers, K_2CO_3, $Pd(PPh_3)_4$, dimethylformamide, and water was subjected to nitrogen degassing for 30 minutes and subsequently heated to 130°C for a duration of 24 hours. After cooling to 25 °C, the mixture was poured into MeOH. The resulting precipitate underwent Soxhlet extraction with MeOH, hexane, and chloroform to eliminate by-products and unreacted materials. The polymers were then collected and subjected to vacuum pressure drying.

ICFTDB.

ICFTBr (238 mg, 0.6 mmol), DB (3,7-bis(4,4,5,5-tetramethyl-1,3,2-dioxaborolan-2-yl)dibenzo[b,d]thiophene 5,5-dioxide, 281 mg, 0.6 mmol), K_2CO_3 (829 mg, 6 mmol), and $Pd(PPh_3)_4$ (69 mg, 0.06 mmol), DMF (24 mL), and water (6 mL) were used for polymerization. Yield: 410 mg.

ICTDB.

ICTBr (111 mg, 0.25 mmol), DB (3,7-bis(4,4,5,5-tetramethyl-1,3,2-dioxaborolan-2-yl)dibenzo[b,d]thiophene 5,5-dioxide, 117 mg, 0.25 mmol), K_2CO_3 (346 mg, 2.5 mmol), and $Pd(PPh_3)_4$ (29 mg, 0.025 mmol), DMF (10 mL), and water (2.5 mL) were used for polymerization. Yield: 120 mg.

IDMTDB.

IDMTBr (492 mg, 1 mmol), DB (3,7-bis(4,4,5,5-tetramethyl-1,3,2-dioxaborolan-2-yl)dibenzo[b,d]thiophene 5,5-dioxide, 468 mg, 1 mmol), K_2CO_3 (1382 mg, 10 mmol), and $Pd(PPh_3)_4$ (116 mg, 0.1 mmol), DMF (40 mL), and water (10 mL) were used for polymerization. Yield: 585 mg.

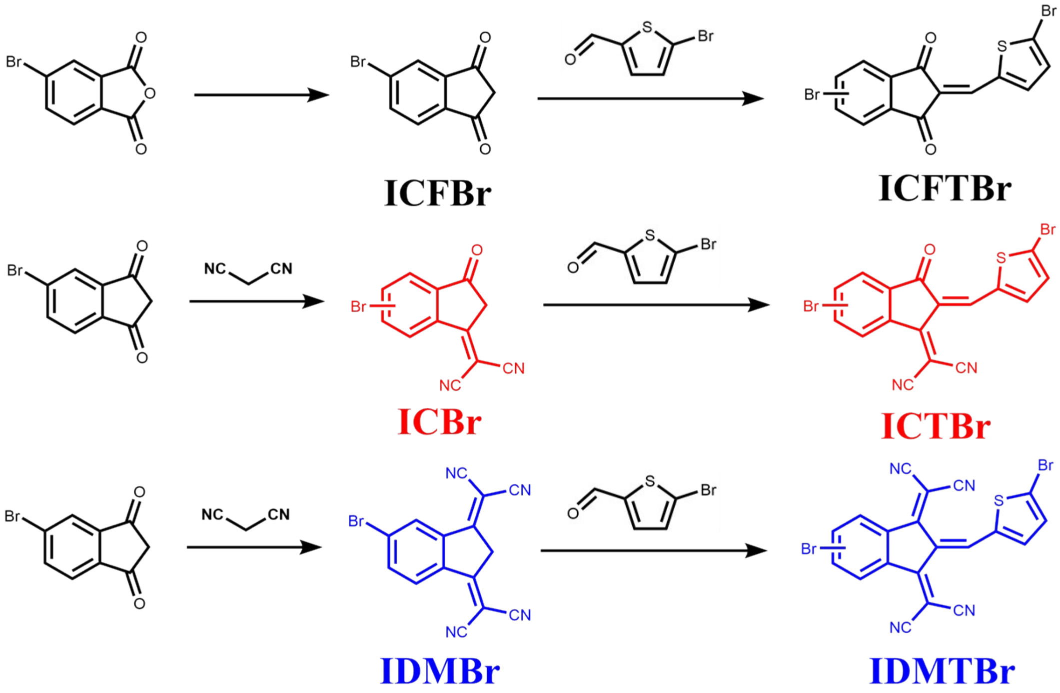

Fig. S1 Synthetic routes for monomers.

Fig. S2 ^{1}H NMR spectra of ICFBr.

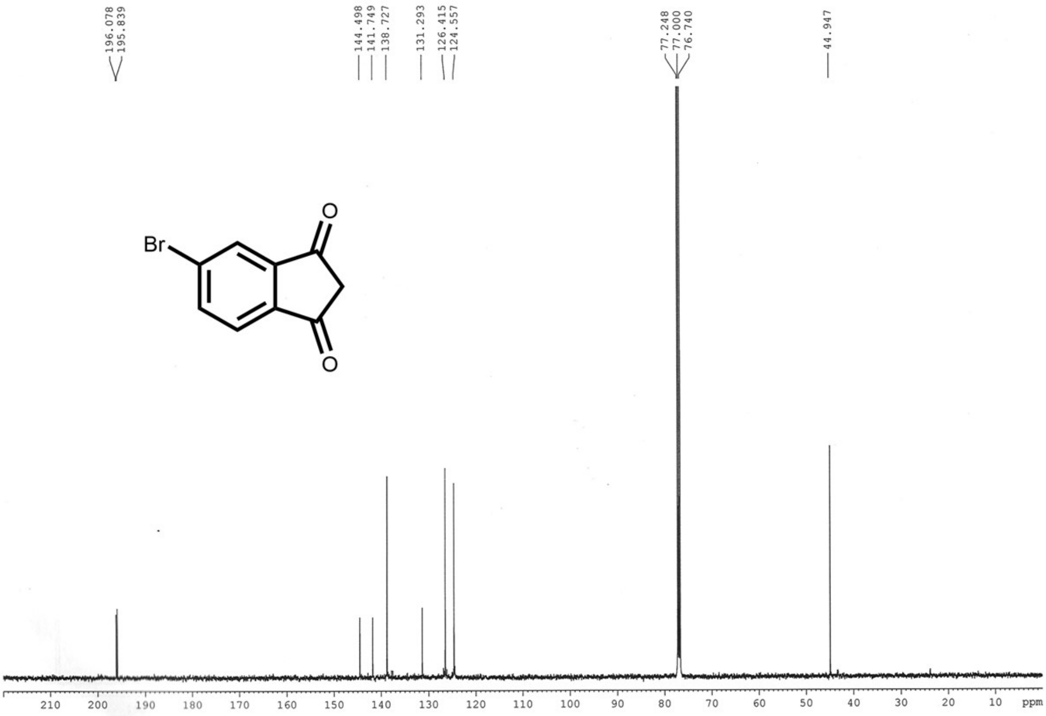

Fig. S3 ^{13}C NMR spectra of ICFBr.

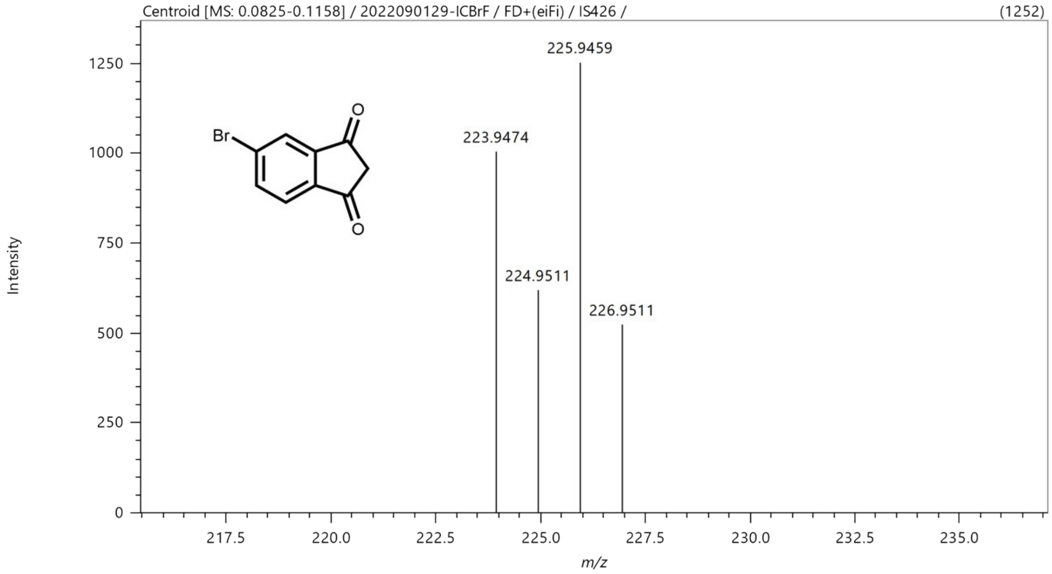

Fig. S4 Mass spectra of ICFBr.

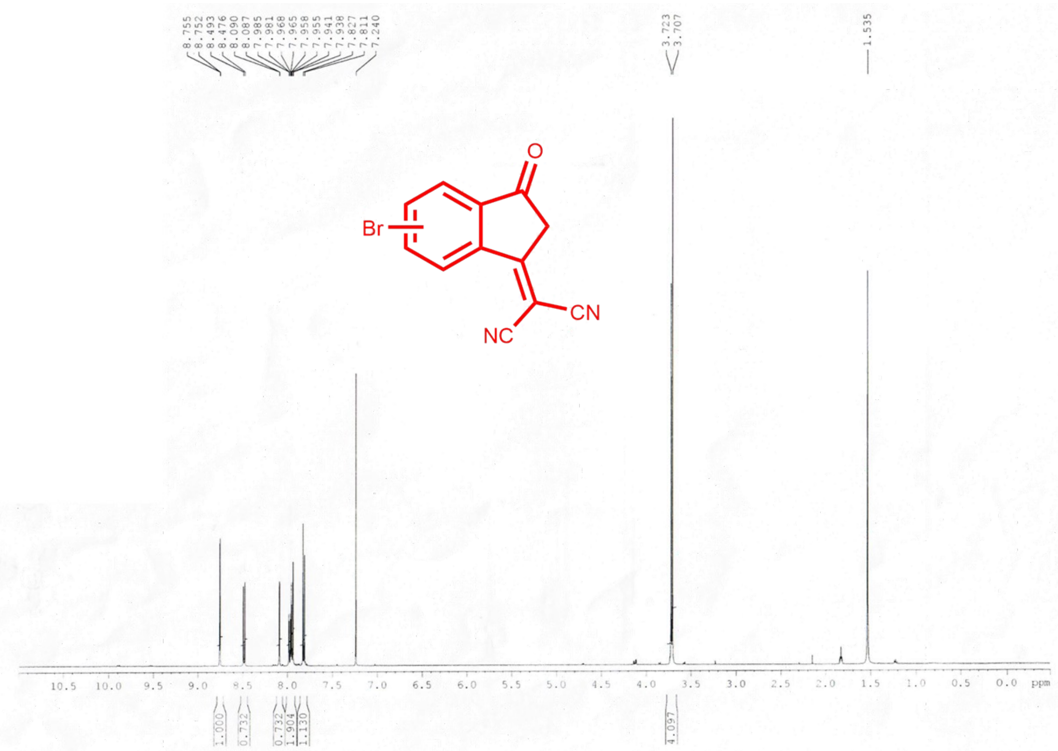

Fig. S5 ^{1}H NMR spectra of ICBr.

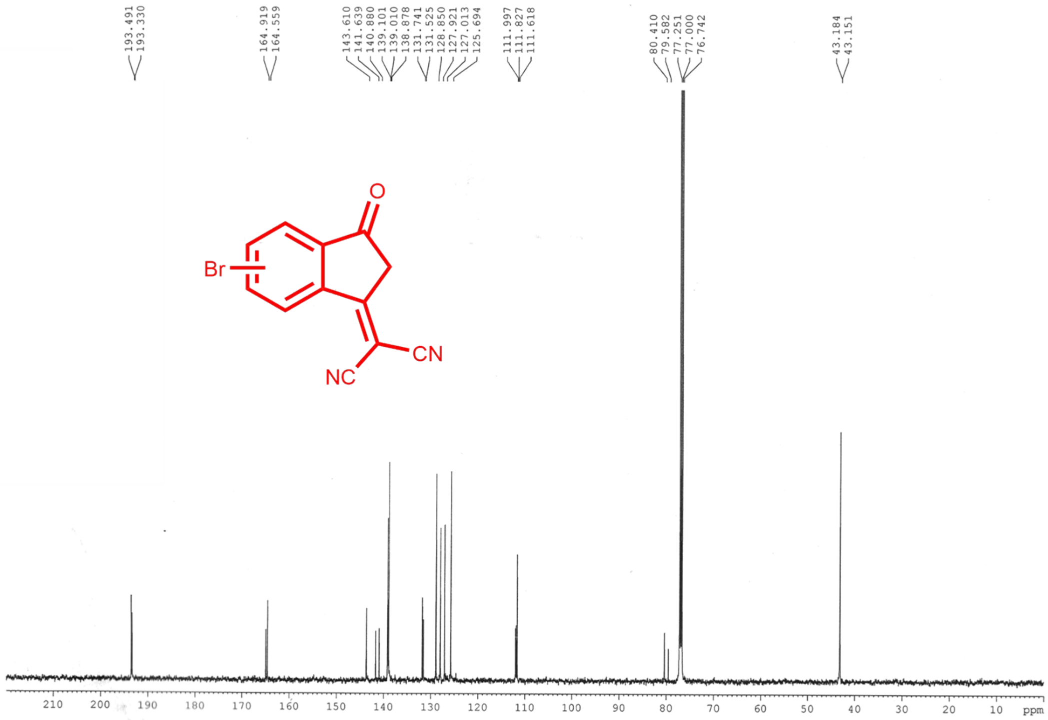

Fig. S6 ^{13}C NMR spectra of ICBr.

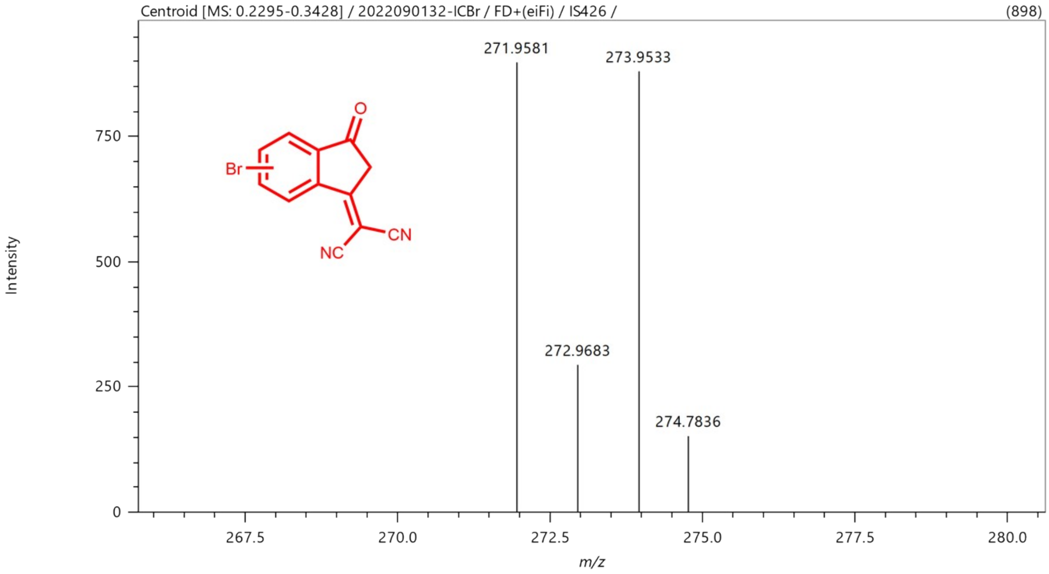

Fig. S7 Mass spectra of ICBr.

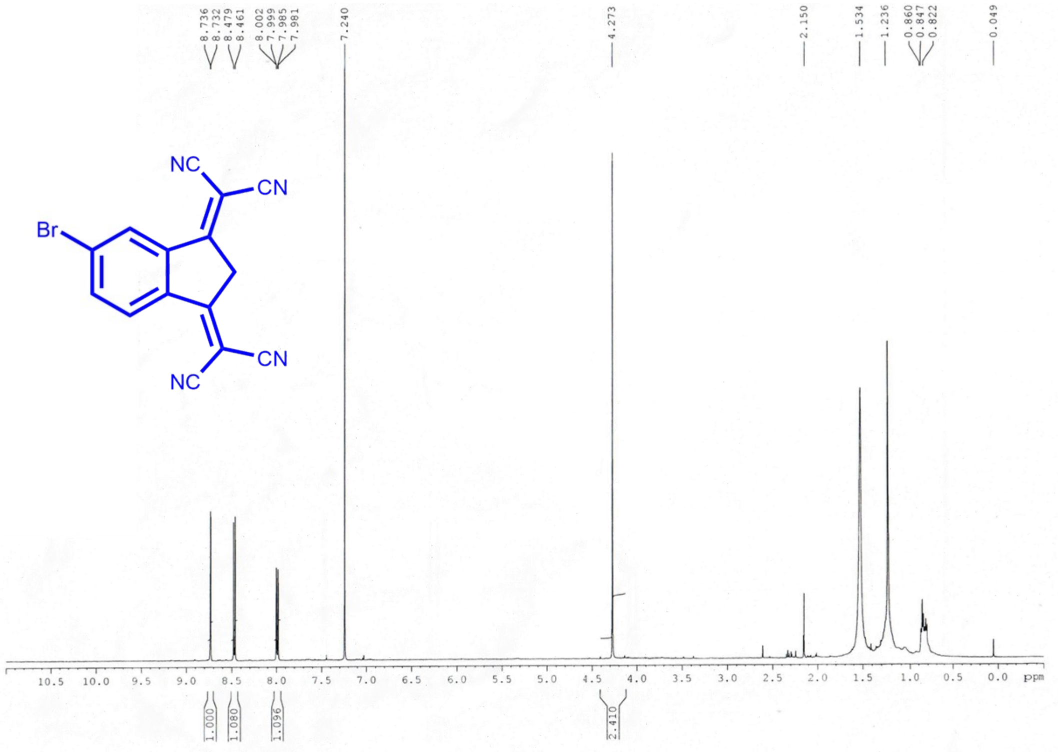

Fig. S8 ^{1}H NMR spectra of IDMBr.

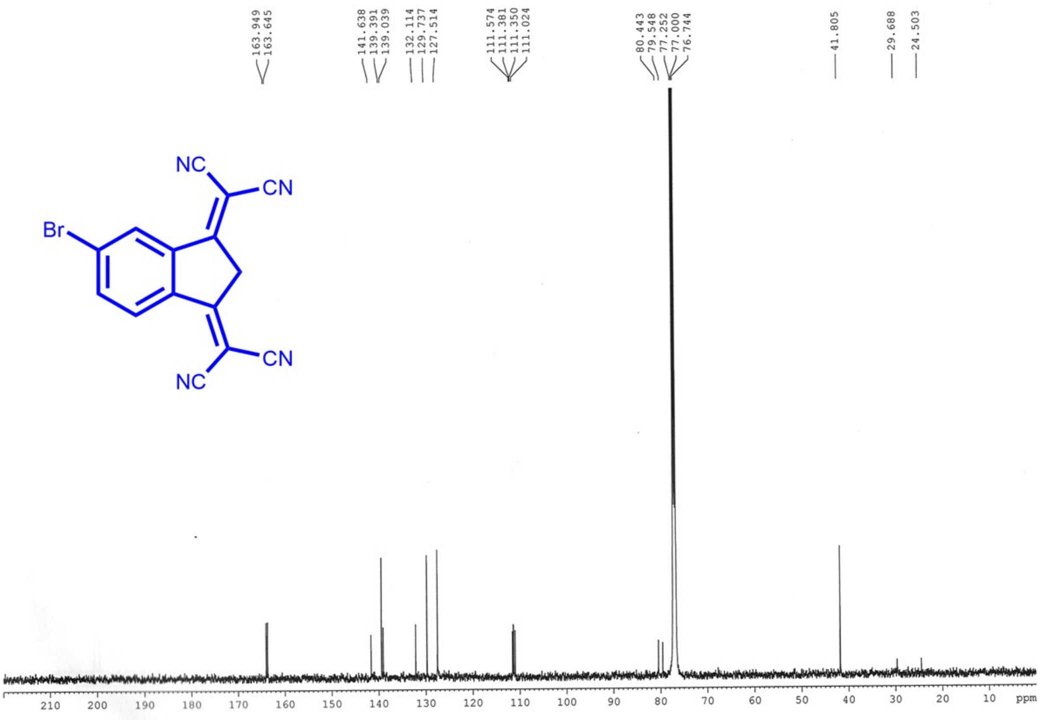

Fig. S9 ^{13}C NMR spectra of IDMBr.

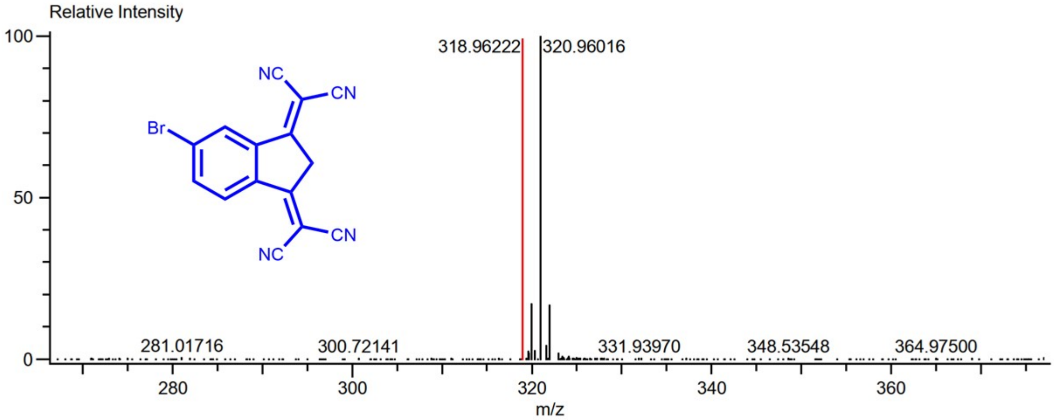

Fig. S10 Mass spectra of IDMBr.

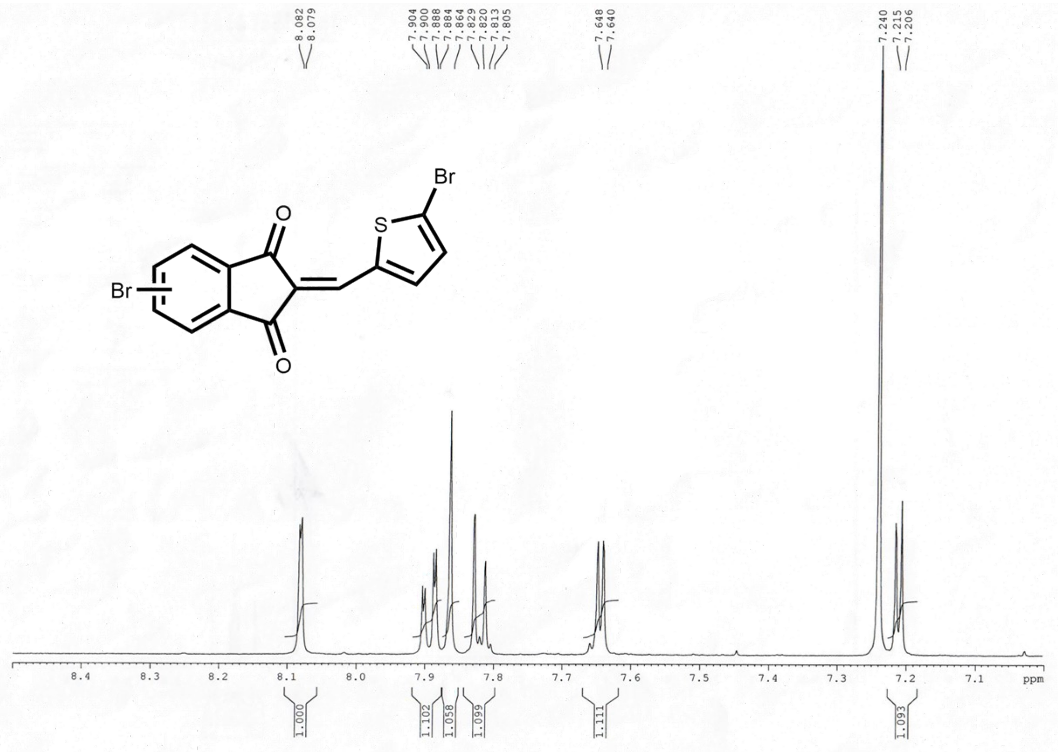

Fig. S11 ^{1}H NMR spectra of ICFTBr.

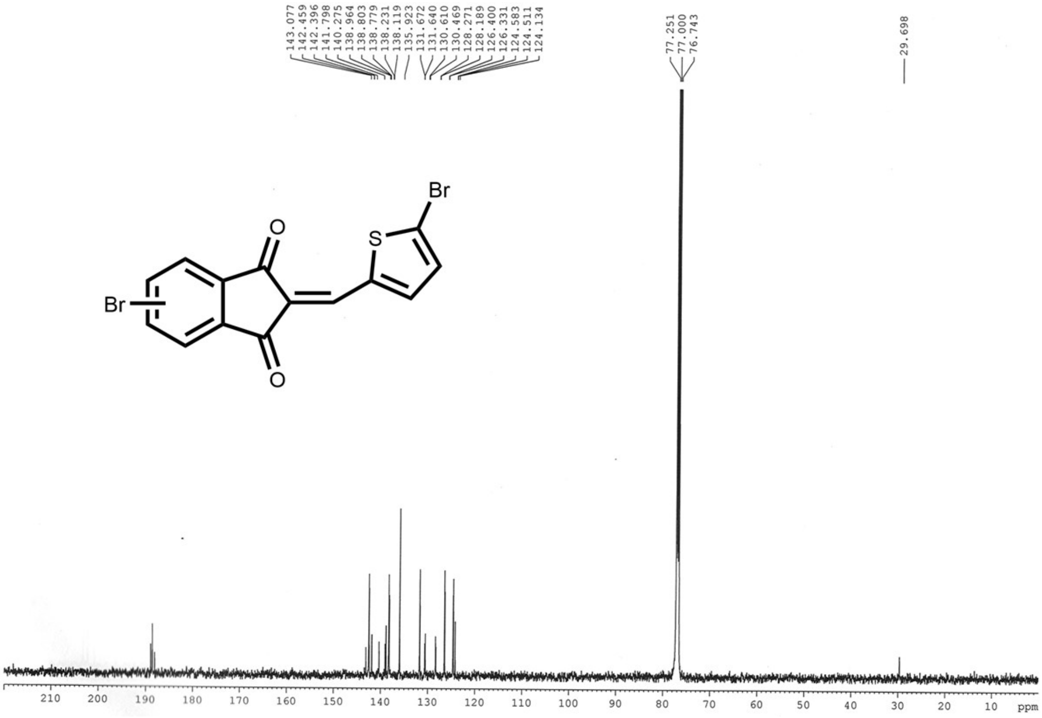

Fig. S12 ^{13}C NMR spectra of ICFTBr.

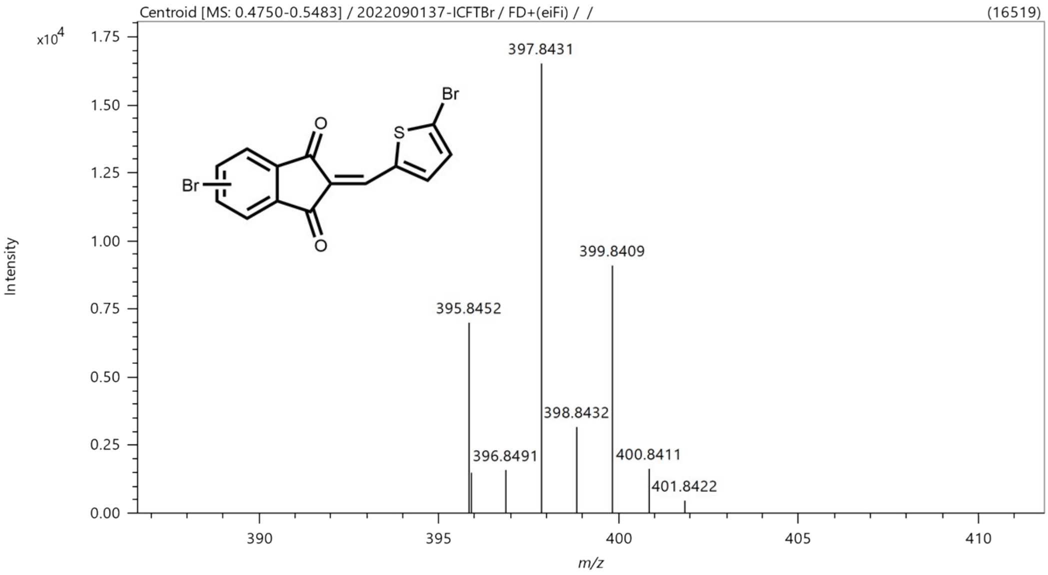

Fig. S13 Mass spectra of ICFTBr.

Fig. S14 ^{1}H NMR spectra of ICTBr.

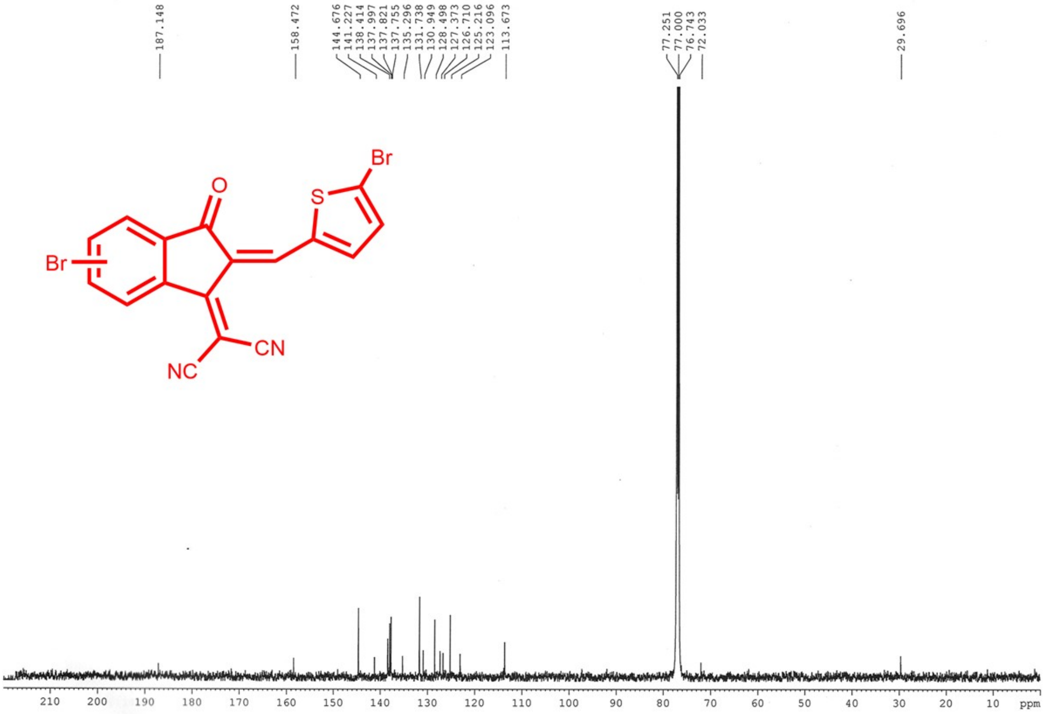

Fig. S15 ^{13}C NMR spectra of ICTBr.

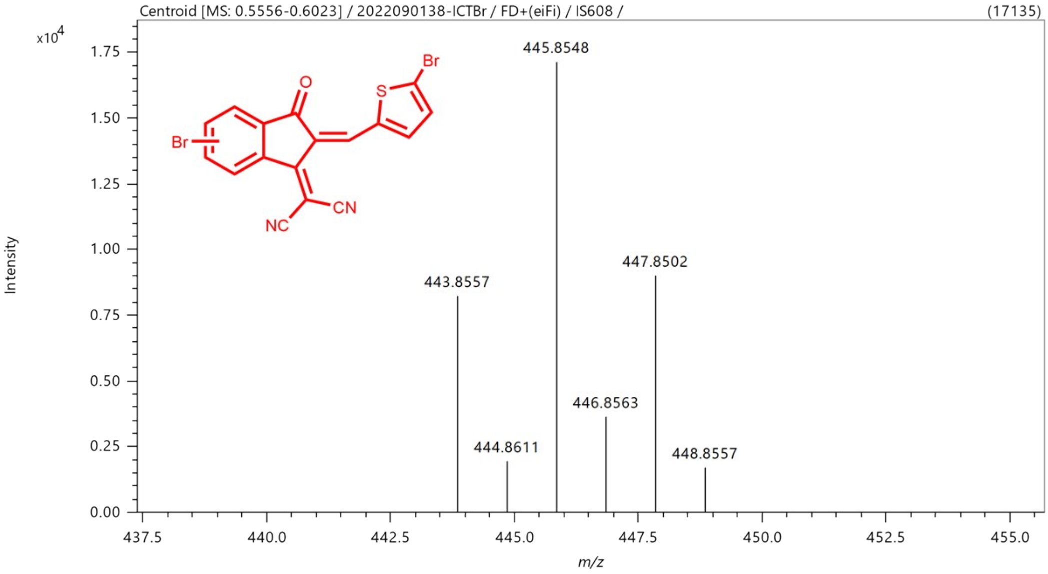

Fig. S16 Mass spectra of ICTBr.

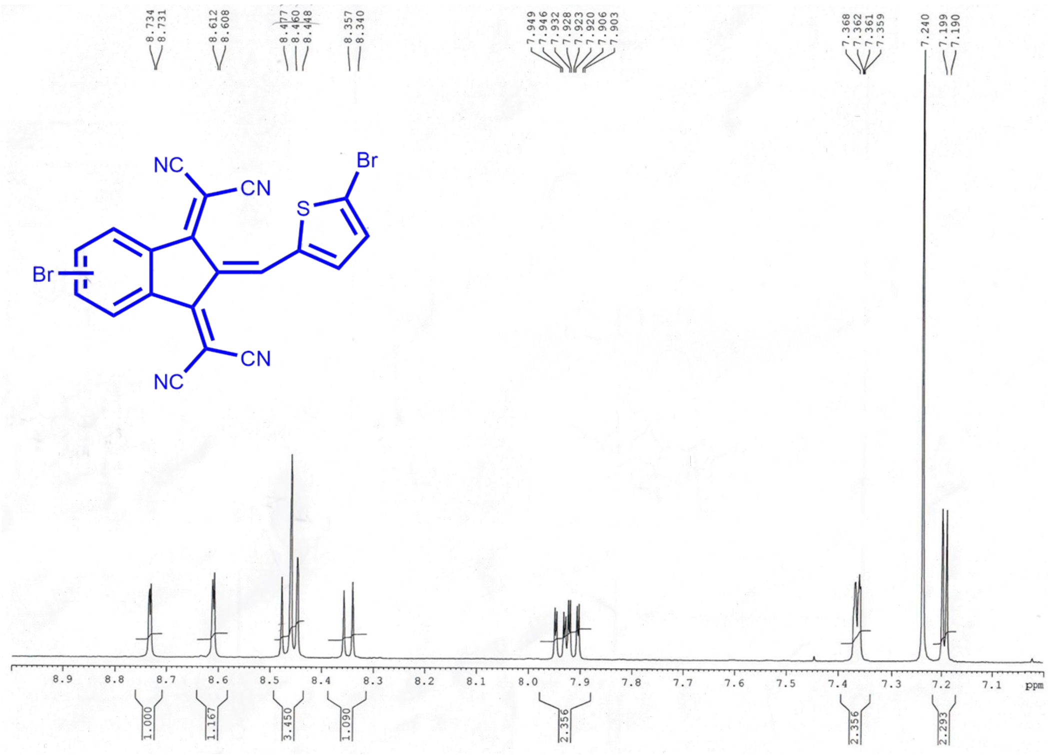

Fig. S17 ^{1}H NMR spectra of IDMTBr.

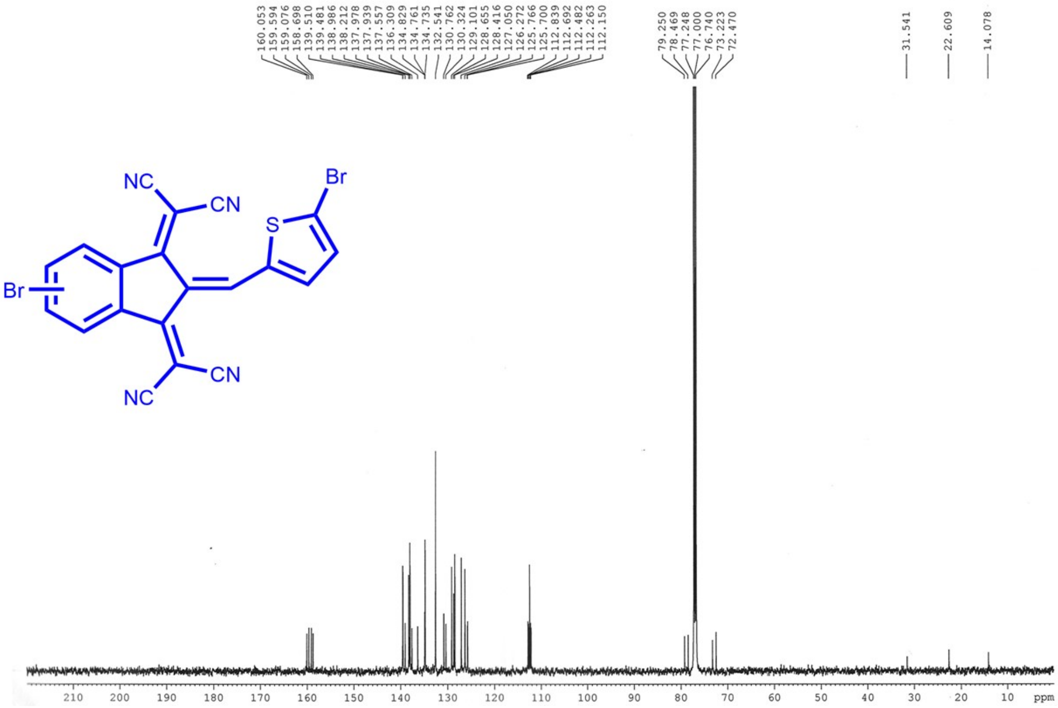

Fig. S18 ^{13}C NMR spectra of IDMTBr.

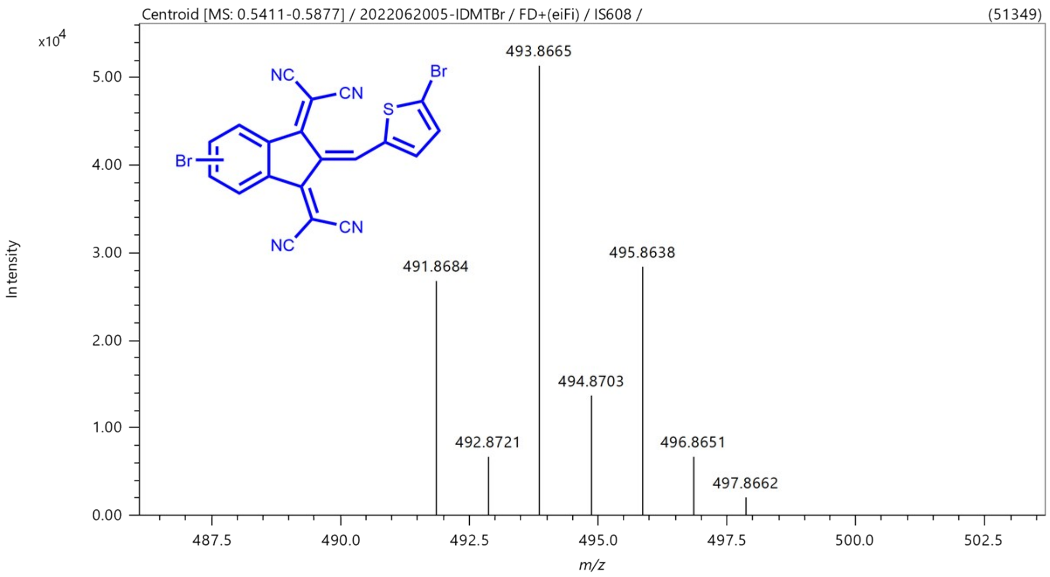

Fig. S19 Mass spectra of IDMTBr.

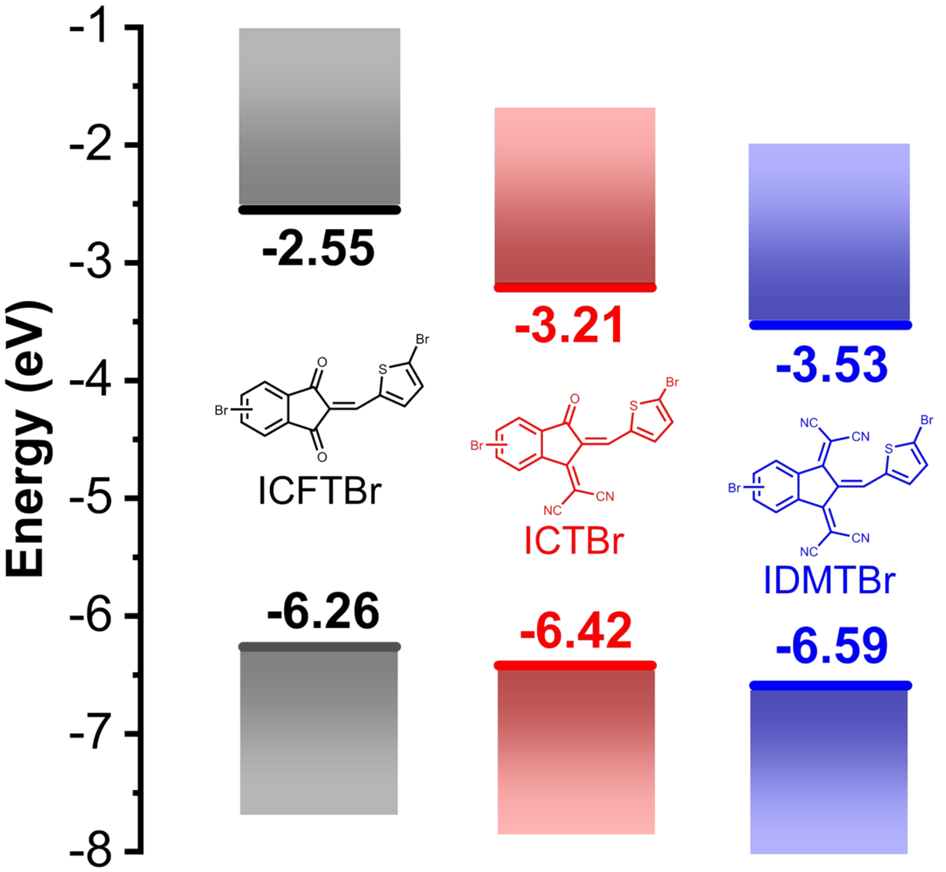

Fig. S20 Calculated LUMO and HOMO energy levels and optical energy gaps of the indanone-based derivatives.

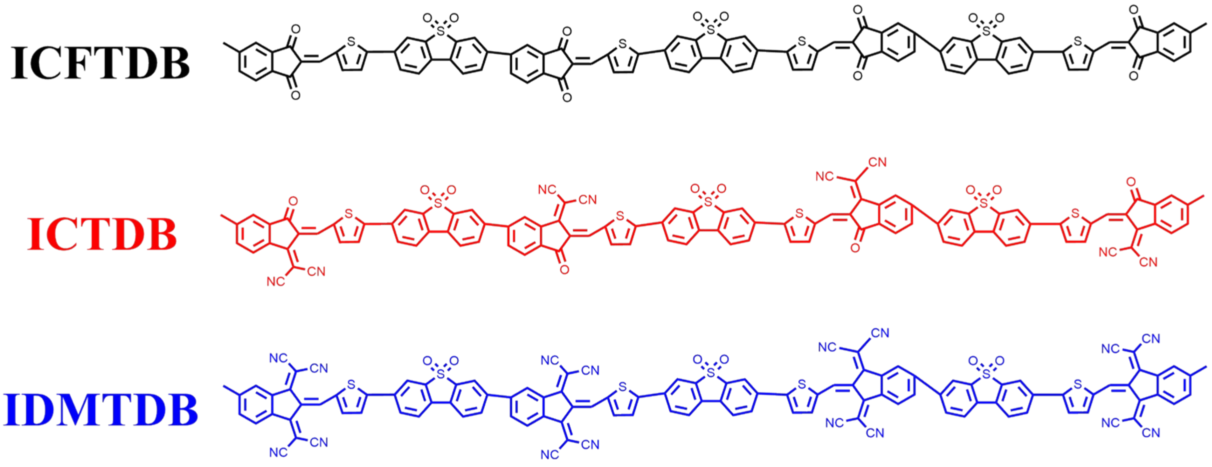

Fig. S21 Molecular structures of indanone-based conjugated polymers.

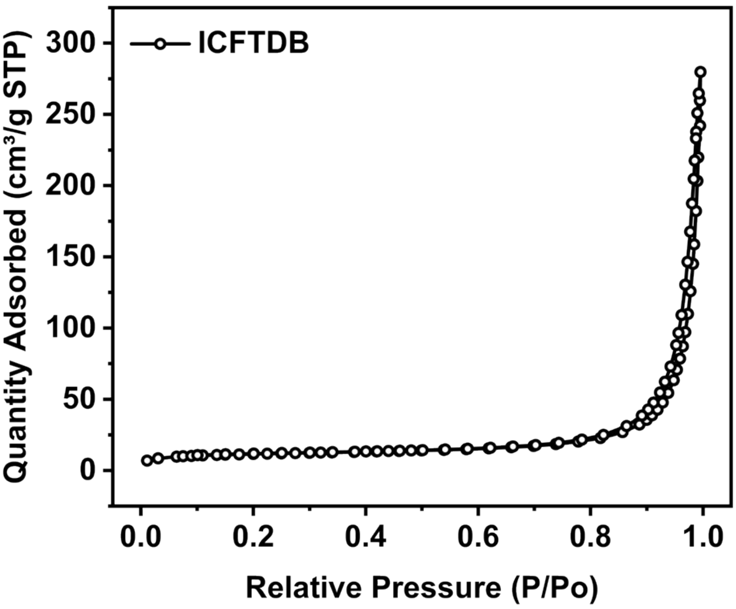

Fig. S22 Brunauer-Emmett-Teller (BET) surface area analysis of ICFTDB.

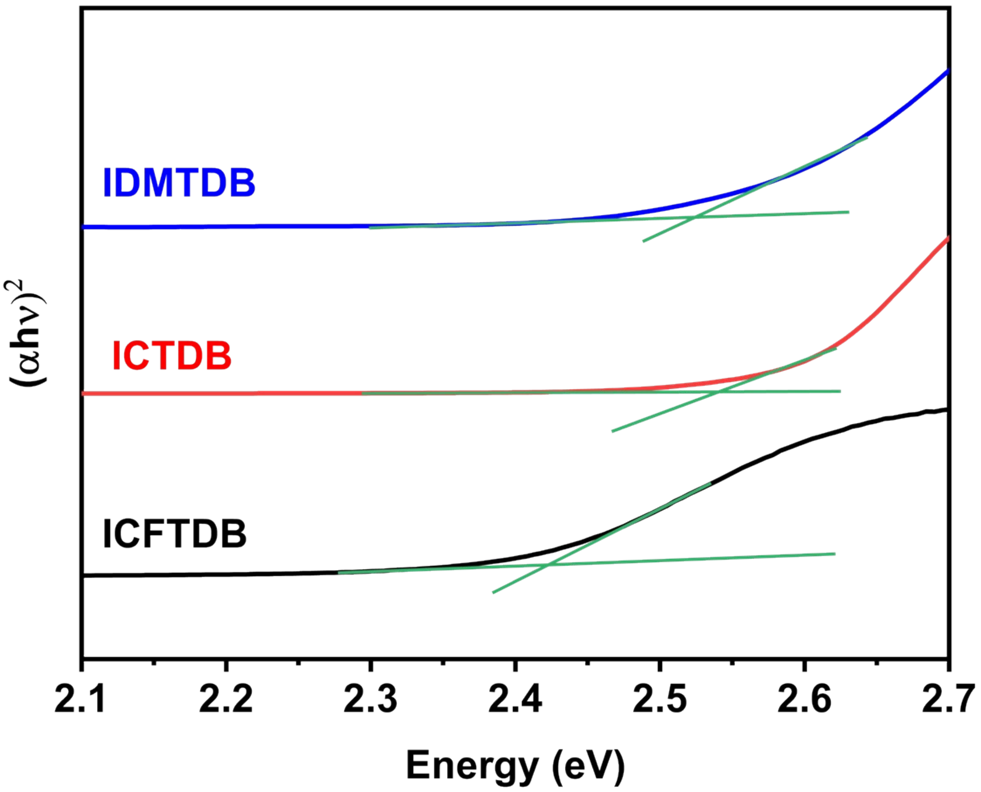

Fig. S23 Tauc plot of indanone-based conjugated polymers.

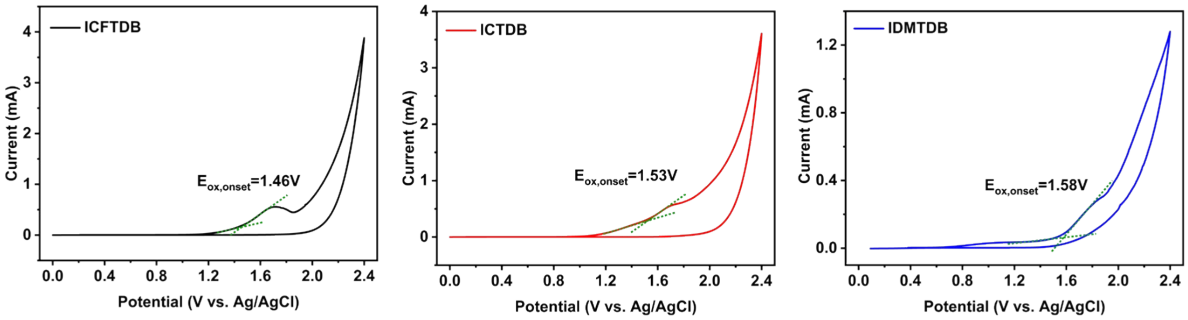

Fig. S24 Cyclic voltammetry measurements of indanone-based conjugated polymers.

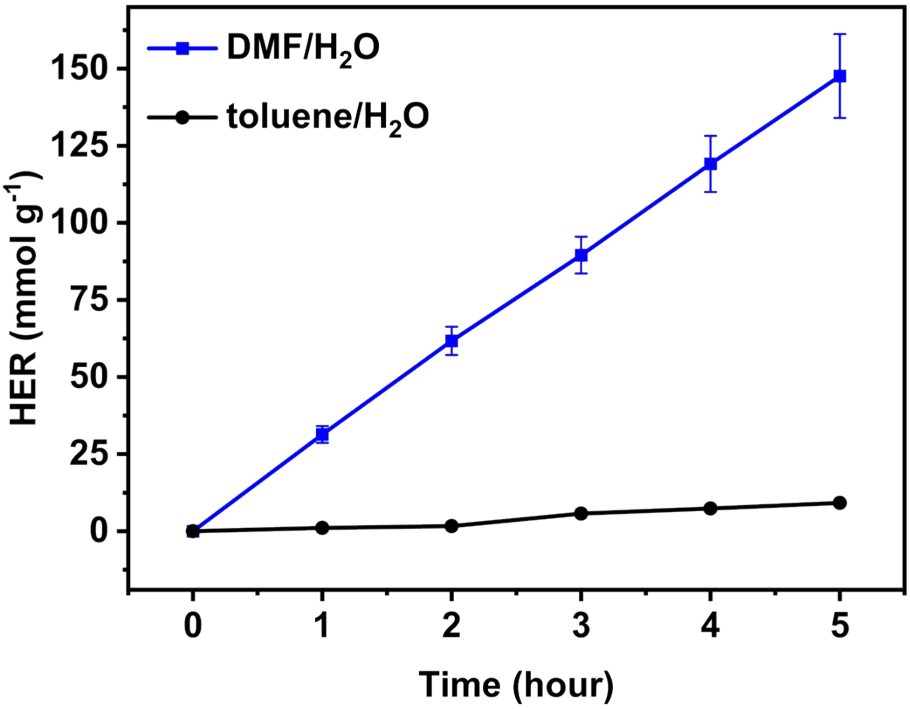

Fig. S25 Optimization of the HER of ICTDB with different polymerization conditions.

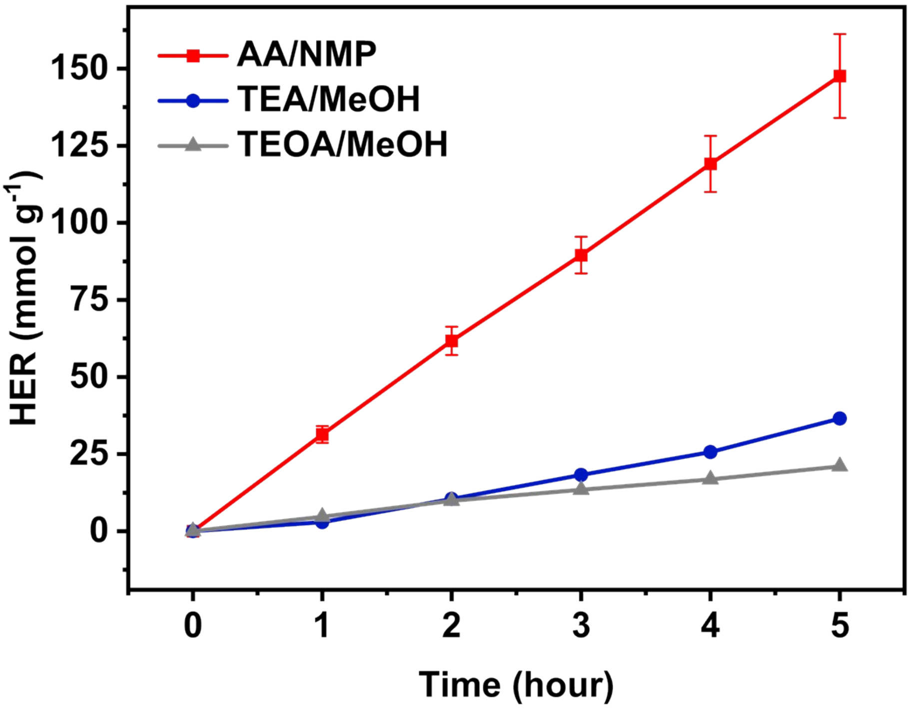

Fig. S26 Optimization of the HER of ICTDB with different sacrificial agents.

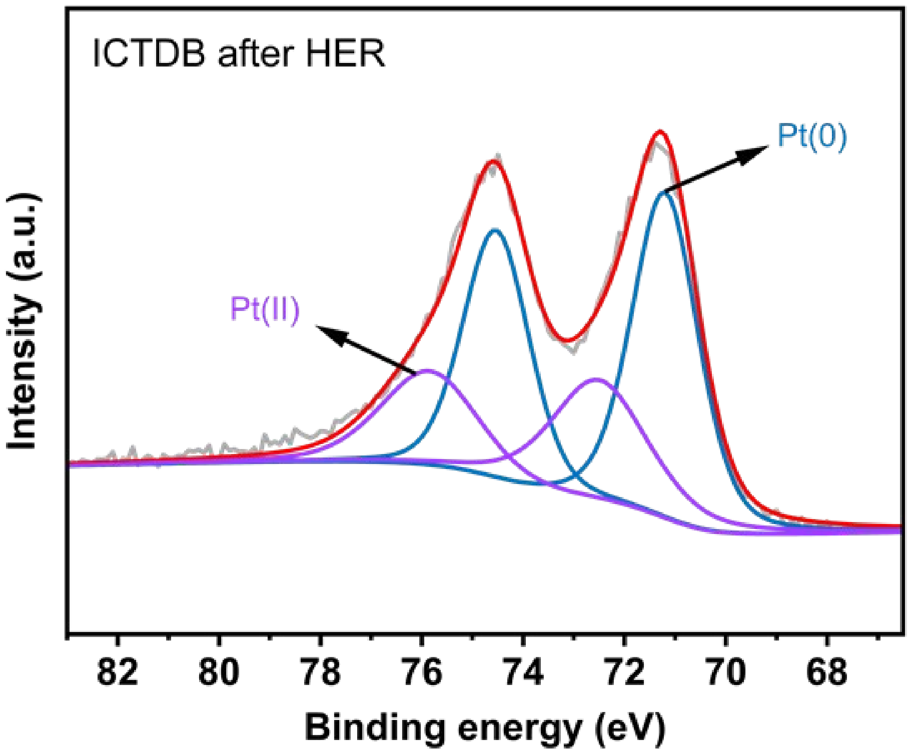

Fig. S27 X-ray photoelectron spectroscopy (XPS) of ICTDB solid powder after HER.

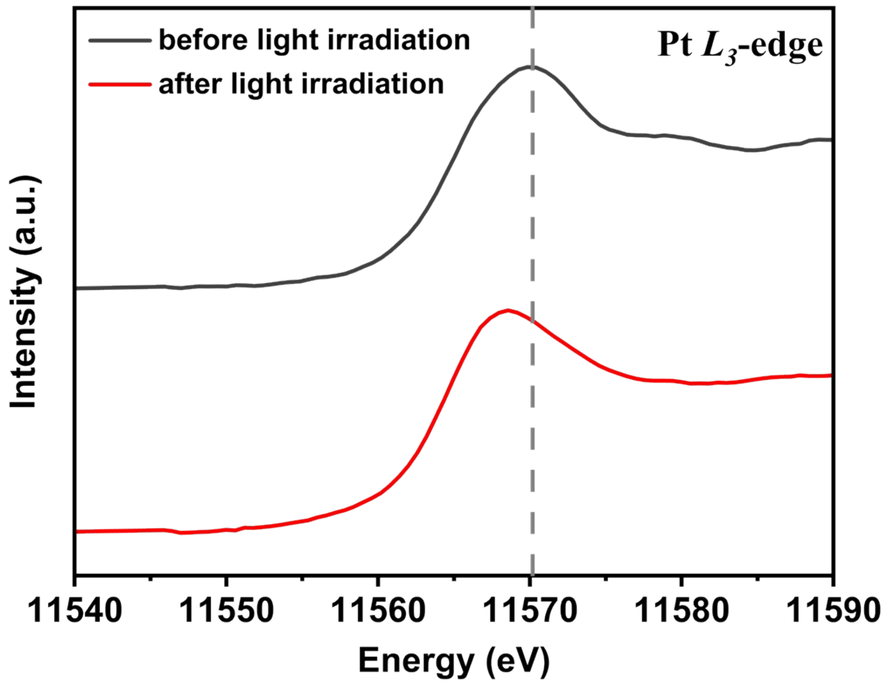

Fig. S28 X-ray absorption spectroscopy (XAS) of ICTDB hydrogen evolution solutions before and after light irradiation.

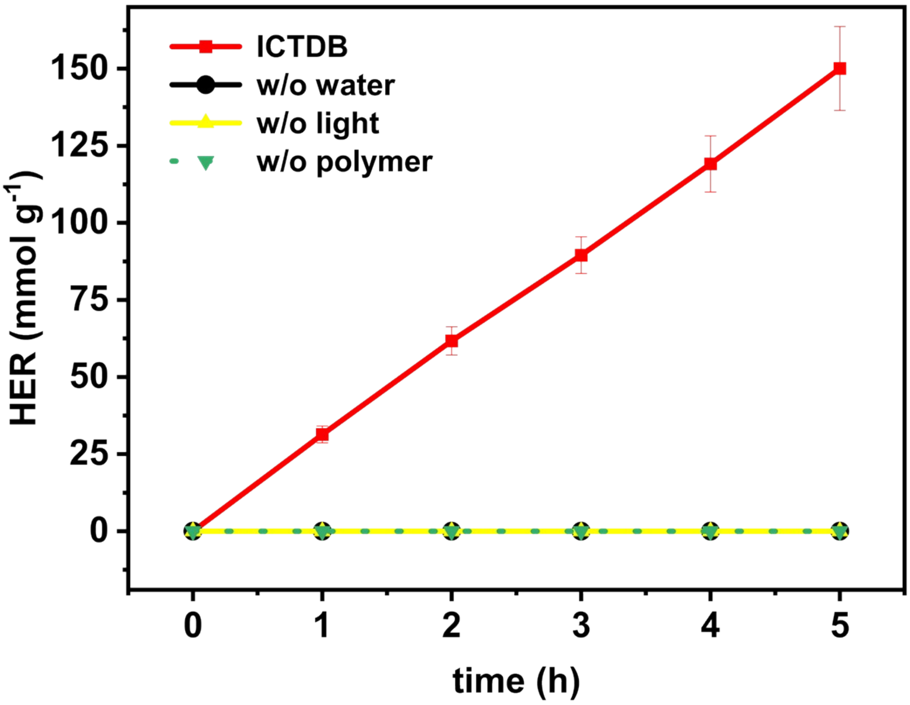

Fig. S29 Control experiment of the HER performance of ICTDB.

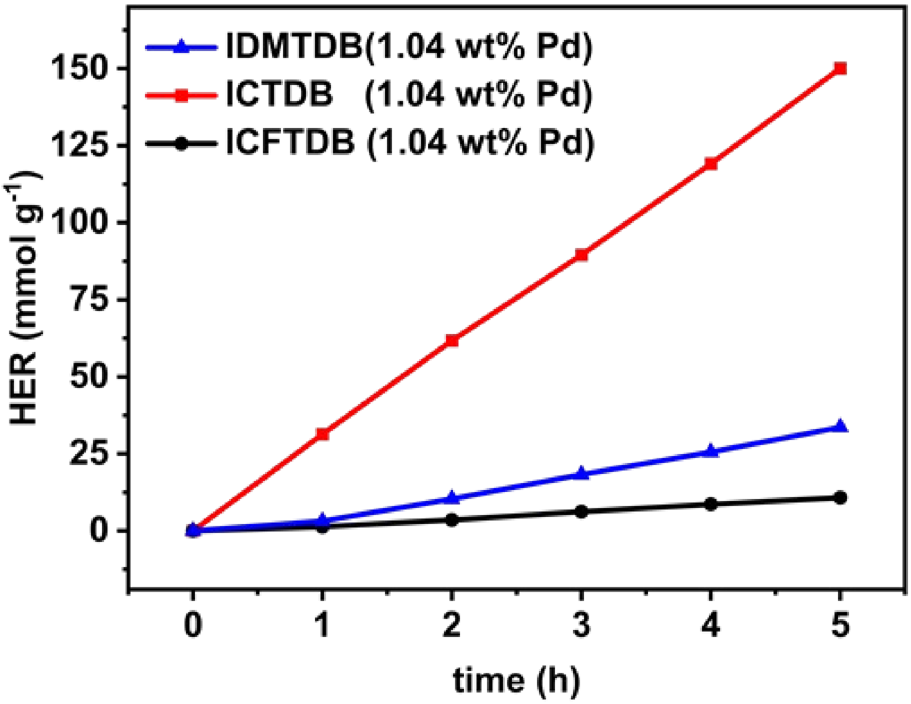

Fig. S30 HER performance of polymers under consistent Pd content levels.

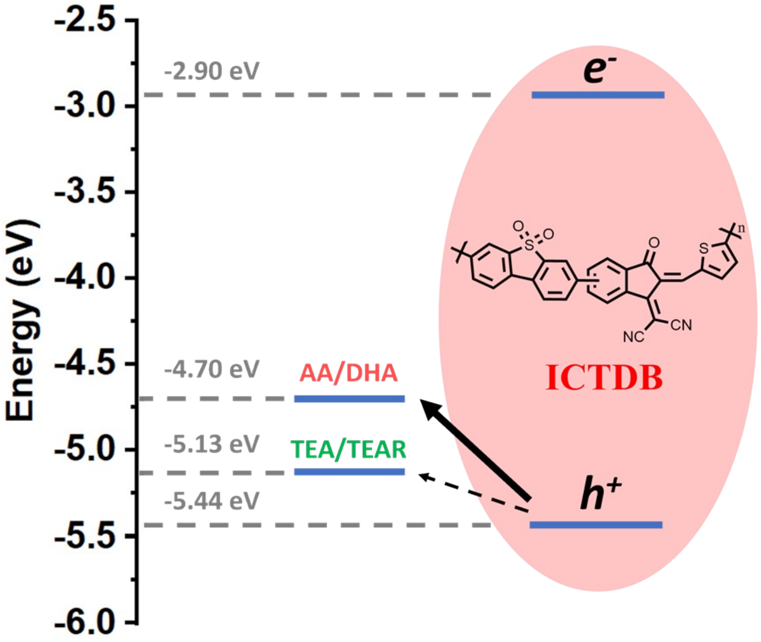

Fig. S31 Relative band positions of ICTDB, and oxidation potential of AA and TEA.

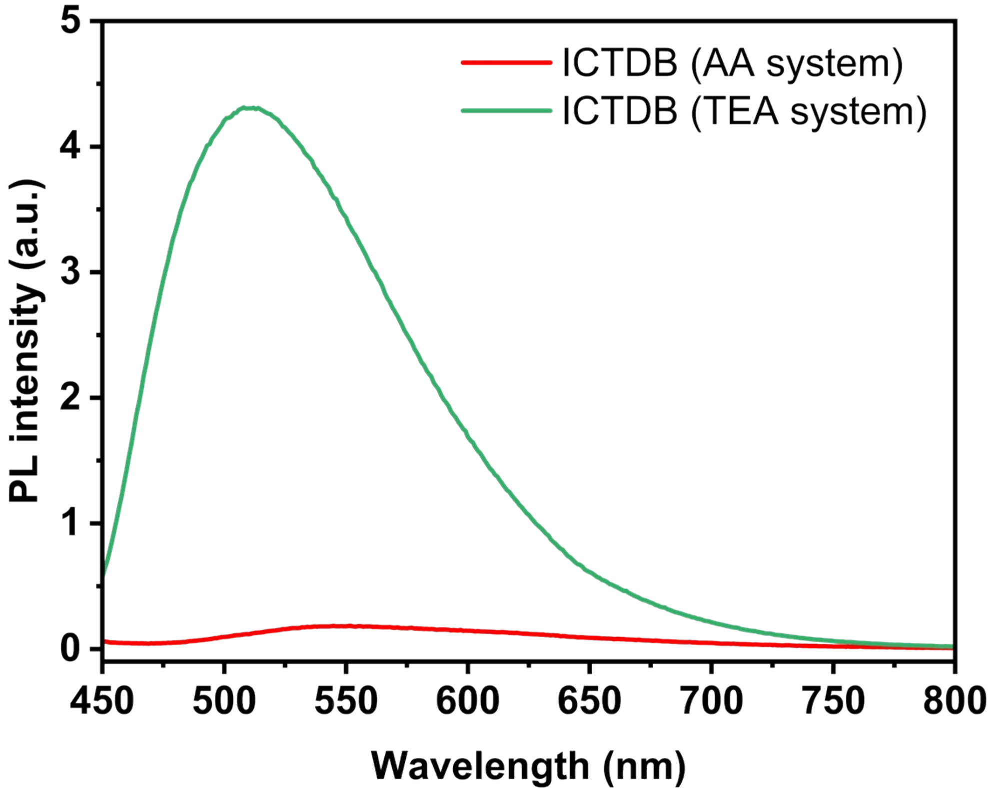

Fig. S32 photoluminescence intensity of ICTDB in AA system and TEA system.

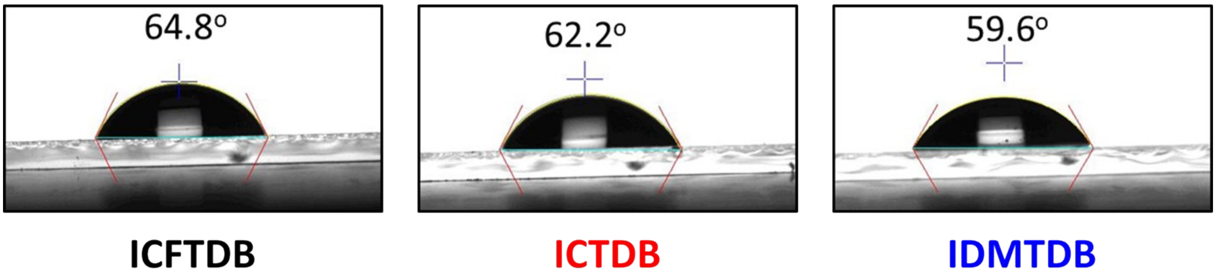

Fig. S33 Water contact angle of the polymers.

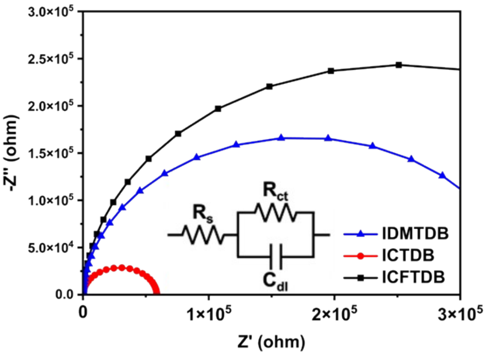

Polymer	$R_s(\Omega)$	$R_{ct}(k\Omega)$
ICFTDB	1512	315.7
ICTDB	1507	31.2
IDMTDB	1499	205.0

Fig. S34 Electrochemical impedance analysis. In the equivalent circuit (inset), R_s represents the circuit series-resistance, R_{ct} is the charge transfer resistance across the interface, and C_{dl} is the capacitance phase element of the semiconductor-electrolyte interface. Simulated R_s and R_{ct} values of polymers for electrochemical impedance test were list in table.

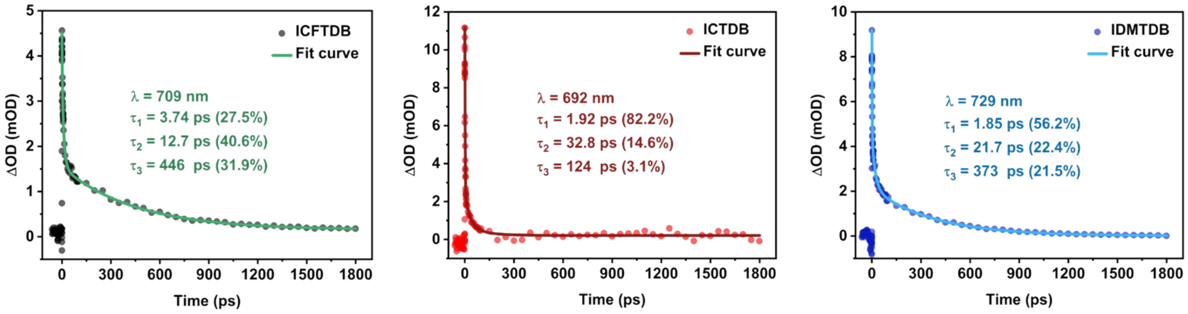

Fig. S35 Fitting curve of TA spectrum of the polymers.

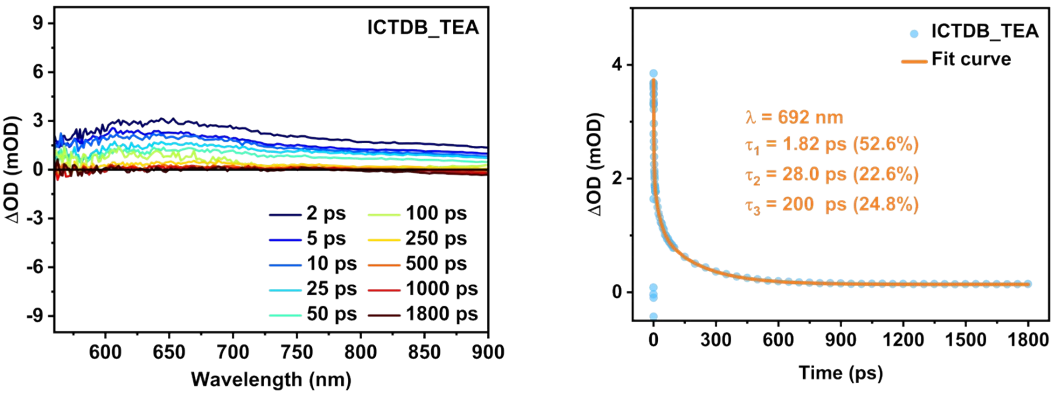

Fig. S36 TA spectra of ICTDB in the TEA system and the corresponding fitting curve.

References

1. W.-C. Lin, J. Jayakumar, C.-L. Chang, L.-Y. Ting, T.-F. Huang, M. H. Elsayed, A. M. Elewa, Y.-T. Lin, J.-J. Liu and Y.-T. Tseng, *J. Mater. Chem. A*, 2022, **10**, 6641-6648.
2. C.-H. Lu, Y.-J. Tsou, H.-Y. Chen, B.-H. Chen, Y.-C. Cheng, S.-D. Yang, M.-C. Chen, C.-C. Hsu and A. H. Kung, *Optica*, 2014, **1**, 400-406.
3. C.-H. Lu, W.-H. Wu, S.-H. Kuo, J.-Y. Guo, M.-C. Chen, S.-D. Yang and A. Kung, *Opt. Express*, 2019, **27**, 15638-15648.
4. Y. C. Wei, B. H. Chen, R. S. Ye, H. W. Huang, J. X. Su, C. Y. Lin, J. Hodgkiss, L. Y. Hsu, Y. Chi and K. Chen, *Angew. Chem. Int. Ed.*, 2023, **62**, e202300815.